HHS Public Access

Author manuscript

Schizophr Res. Author manuscript; available in PMC 2017 February 01.

Published in final edited form as:

Schizophr Res. 2016 February ; 170(0): 235–244. doi:10.1016/j.schres.2015.12.016.

NeuN+ Neuronal Nuclei in Non-Human Primate Prefrontal Cortex and Subcortical White Matter After Clozapine Exposure

Tobias B. Halene, MD PhD[1,*], **Alexey Kozlenkov, PhD**[1], **Yan Jiang, PhD**[1], **Amanda Mitchell, PhD**[1], **Behnam Javidfar**[1], **Aslihan Dincer, MS**[1], **Royce Park**[1], **Jennifer Wiseman**[1], **Paula Croxson, PhD**[3], **Eustathia Lela Giannaris, PhD**[2], **Patrick R. Hof, MD**[3], **Panos Roussos, MD PhD**[1,4], **Stella Dracheva, PhD**[1], **Scott E. Hemby, PhD**[5,#], and **Schahram Akbarian, MD PhD**[1]

[1]Department of Psychiatry, Icahn School of Medicine at Mount Sinai, New York, NY, USA

[2]Department of Cell and Developmental Biology, University of Massachusetts Medical School, Worcester, MA, USA

[3]Fishberg Department of Neuroscience and Friedman Brain Institute, Icahn School of Medicine at Mount Sinai, New York, NY, USA

[4]Department of Genetics and Genomic Science and Institute for Multiscale Biology, Icahn School of Medicine at Mount Sinai, New York, NY, USA

[5]Department of Physiology and Pharmacology, Wake Forest University, Winston-Salem, NC, USA

Abstract

Increased neuronal densities in subcortical white matter have been reported for some cases with schizophrenia. The underlying cellular and molecular mechanisms remain unresolved.

We exposed 26 young adult macaque monkeys for 6 months to either clozapine, haloperidol or placebo and measured by structural MRI frontal gray and white matter volumes before and after treatment, followed by observer-independent, flow-cytometry-based quantification of neuronal and non-neuronal nuclei and molecular fingerprinting of cell-type specific transcripts.

[*]Corresponding author: Tobias B. Halene, MD PhD, Icahn School of Medicine at Mount Sinai, Department of Psychiatry, 1470 Madison Ave, Hess 9-105, New York, NY 10029, Tel: 646 627 5529, Fax: 646-537-9583, tobias.halene@mountsinai.org.
[#]Present address:
Department of Basic Pharmaceutical Sciences, Highpoint University, 833 Montlieu Ave, NC 27262

Contributors

Schahram Akbarian and Scott Hemby developed the idea and wrote this article with Tobias Halene who was also responsible for flow-cytometry (with Alexey Kozlenkov and Stella Dracheva), MRI image processing and analysis (with Paula Croxsom) and RT-PCR (with Amanda Mitchell and Yan Jiang. Aslihan Dincer provided RNA-seq tracks, Patrick Hof and also Behnam Javidfar conducted immunohistochemical experiment and provided immunofluorescence confocal microscopy images, Eustathia Lela Giannaris conducted pilot studies on white matter NeuN nuclei staining and counting, Jennifer Weisman and Royce ParkPanos Roussos provided statistical analysis. Scott Hemby was also responsible for treatment, imaging and necropsies. All authors contributed to and have approved the final manuscript.

Disclosure:

Conflict of interest

The authors have no conflict of interest to declare.

After clozapine exposure, the proportion of nuclei expressing the neuronal marker NeuN increased by approximately 50% in subcortical white matter, in conjunction with a more subtle and non-significant increase in overlying gray matter. Numbers and proportions of nuclei expressing the oligodendrocyte lineage marker, OLIG2, and cell-type specific RNA expression patterns, were maintained after antipsychotic drug exposure. Frontal lobe gray and white matter volumes remained indistinguishable between antipsychotic-drug-exposed and control groups.

Chronic clozapine exposure increases the proportion of $NeuN^+$ nuclei in frontal subcortical white matter, without alterations in frontal lobe volumes or cell type-specific gene expression. Further exploration of neurochemical plasticity in non-human primate brain exposed to antipsychotic drugs is warranted.

Introduction

Schizophrenia, a major psychiatric disorder significantly impacting quality of life, is commonly treated with antipsychotic drugs but many patients show insufficient responses to current treatments (Lieberman et al., 2005; Swartz et al., 2007). Therefore, the pursuit of new schizophrenia treatments should start, among other approaches, with detailed explorations of transcriptomes (Feher et al., 2005; Girgenti et al., 2010; Iancu et al., 2012; Middleton et al., 2002) and synaptic proteomes (Ji et al., 2009; Ma et al., 2009) in brains exposed to typical dopamine D_2-preferential antagonists and atypical antipsychotic drugs with broader receptor profiles. Changes in cell composition of the antipsychotic-drug-exposed brain have also been reported. Long-term exposure of non-human primates to two widely prescribed antipsychotics, haloperidol and olanzapine, resulted in 8–11% brain weight reduction and volume loss affecting gray and white matter, decreased astro- and oligodendrocyte numbers (Konopaske et al., 2008), together with a 10.2% increase in neuronal densities (Konopaske et al., 2007).

These findings are also of interesting from the viewpoint of the interstitial white matter neurons (WMN), a cell type residing in subcortical white matter of the adult brain. The large majority of WMN are considered remnants of the subplate, a transient structure important for connectivity formation during early development(Kanold, 2004; Kostovic et al., 2011). Interestingly, more than 15 studies have examined post-mortem brain tissue and reported supernormal WMN numbers and densities in prefrontal, cingulate and medial or lateral temporal cortex of subjects diagnosed with schizophrenia(Akbarian et al., 1993a; Akbarian et al., 1996; Akbarian et al., 1993b; Anderson et al., 1996; Eastwood and Harrison, 2003, 2005; Ikeda et al., 2004; Joshi et al., 2012; Kirkpatrick et al., 1999; Kirkpatrick et al., 2003; Rioux et al., 2003; Yang et al., 2011). While negative findings have also been published (Beasley et al., 2002; Beasley et al., 2009) most research on this topic indicates that WMN alterations could affect a subset of up to 25% of patients with schizophrenia(Connor et al., 2009). It remains unclear whether increased numbers of WMN in patients with schizophrenia marks a subtype of schizophrenia and if treatment with antipsychotic medication *in vivo* plays any role. So far, medication-induced changes in WMN never have been explored in a controlled, prospective study. This is both surprising, given the potential importance of antipsychotic drugs, which are widely prescribed to millions of patients, and

anticipated, as controlled studies on drug-mediated effects very difficult to conduct on human brain.

Here, we designed an integrative study on 26 macaque monkeys subjected to 6 months of oral intake of haloperidol and clozapine, followed by MRI-based *in vivo* neuroimaging with scans before and after antipsychotic drug exposure, followed by automated quantification of neuron to glia (non-neuron) ratios in frontal gray and white matter and cell-type specific molecular fingerprinting (Figure 1). We choose haloperidol and clozapine because these drugs are extensively prescribed prototypes representing conventional antipsychotics primarily acting as dopamine D_2 receptor antagonists (haloperidol) or atypical antipsychotics with broader receptor profiles (clozapine). Furthermore, clozapine is generally considered of superior therapeutic efficiency compared to many of the typical or atypical antipsychotics(Meltzer, 2013; Wenthur and Lindsley, 2013). We report increased proportions of nuclei expressing the neuronal phenotypic marker for '*Neuronal Nuclei*' (NeuN)(Mullen et al., 1992) after clozapine exposure, affecting subcortical white matter and more subtle changes in overlying cortex, without affecting cortical volumes or cell type specific gene expression.

Materials and Methods

Animals and antipsychotic drug treatments

26 young adult and drug-naïve rhesus macaques (12 female, 14 male) were randomly assigned to one of three treatment groups: haloperidol (4 mg/kg/day), clozapine (5.2 mg/kg/day), or vehicle (Table 1). Using previously established protocols (Lidow et al., 1997; Lidow and Goldman-Rakic, 1994, 1997), monkeys were administered antipsychotic drugs orally for six months, mixed with powdered sugar and given in peanut butter or fruit treats. Monkeys received standard enrichment, including social enrichment, human interaction, variety in diet, and age-appropriate objects as directed by the Animal Welfare Act and the Wake Forest University Policy for Non-human Primate Environmental Enrichment. Animal care procedures strictly followed the National Institutes of Health Guide for the Care and Use of Laboratory Animals and were approved by the Institutional Animal Care and Use Committee of Wake Forest Health Sciences. All 26 animals completed the treatment.

MRI/ Neuroimaging

In vivo imaging studies were conducted on altogether 18 of the 26 animals. Scans from one animal were excluded for technical reasons, leaving 5 controls, 7 haloperidol- and 5 clozapine-treated animals for imaging analyses. Each animal was scanned twice, immediately before the first drug (or vehicle) treatment and again 2 weeks before necropsy. Drug treatment continued until the day of necropsy. Images were acquired on a General Electric 3.0 Tesla Signa MR unit (GE Healthcare Systems) with a human GE quadrature lower extremity coil. During the scanning procedure, the monkeys were anesthetized with 6 mg/kg i.m. of Telazol® (Aveco) and 0.05–0.1 mg/kg i.m. of Acepromazine (Ayerst,), and placed in a MRI-compatible head holder. Following a conventional sagittal scout scan (TR=500 ms, TE=12 ms, flip angle=90°), a three-dimensional Inversion Recovery Prepared T_1-weighted spoiled gradient echo (SPGR) protocol was used to acquire structural brain

images (TR=14 ms, TI=300 ms, TE=3 ms, flip angle=15°, number of averages=4, acquisition matrix=256×256). The SPGR scan contained 124 contiguous transaxial slices of 0.5 mm thickness (with no inter-slice gap) through the entire brain.

Image processing and analysis

Image segmentation and analysis routines were performed using standard statistical parametric mapping techniques along with customized scripts in MATLAB 6.5 (Mathworks). The 124 transaxial slices from the SPGR scan were converted into Analyze format and resized to yield isotropic voxels of 0.47 mm^3. The image volumes associated with each animal were oriented to the anterior-posterior commissural plane to eliminate slice angle bias.

Image analysis

Skull stripping and tissue-type segmentation was performed, using tools from the Oxford Centre for Functional Magnetic Resonance Imaging of the Brain's Software Library (FMRIB; www.fmrib.ox.ac.uk/~fsl). Brains were first extracted using FMRIB's Brain Extraction Tool(Smith, 2002). The output binary mask was adjusted in FSL View. Smoothed and skull-stripped images were created for all three co-registered images (T1, T2, PD). Binary masks and stripped images were also created for the frontal target area for each monkey using the predefined frontal target area according to the anatomical criteria described below. An automated segmentation tool (FAST) was used to perform probabilistic tissue-type segmentation and partial volume estimation for the frontal target area into different tissue types (gray, white matter, cerebrospinal fluid) (Zhang et al., 2001). Masks, averaging output and skull stripped images were visually inspected to check the accuracy and anatomical plausibility of masks averages and volume estimates. Partial volume estimate files generated by FAST were used to calculate voxel volumes for tissue types pre and post treatment. To determine whether calculated voxel volumes were statistically different between groups (treatment; before and after treatment), gray and white matter voxel volumes were compared using repeated-measures ANOVAs. The definition of prefrontal target area was based on sulci that were easily and reliably identified on MRI scans. Our region-of-interest for the volumetric measurements was defined as the area between frontal poles (anterior border), arcuate sulci (posterior border) and superior up to the horizontal plane where the two orbital sulci could no longer be clearly defined. This area would cover the biopsy sites of that would follow after necropsy and provide tissue for fluorescence-activated nuclei counting.

Tissue dissection and fluorescence-activated nuclei counting

After the last drug administration, monkeys were sedated with ketamine (10 mg/kg; IM), followed by sodium pentobarbital overdose, then transcardially perfused with ice-cold phosphate-buffered saline. Brains were removed and cut into 4 mm-thick coronal slabs, which aids in the dissection of discrete brain regions, allowing slicing of repeatable sections of the monkey brain. Subsequently, samples were frozen on dry ice and stored at −80°C. The post mortem interval, i.e. the time from heart puncture for perfusion to freezing the last piece of tissue was less than 40 minutes for all monkeys. For the brain biopsies needed for the downstream experiments, brain tissue was excised with a Miltex 3.5 mm diameter short

handle biopsy puncher. Care was taken to maximize consistency of the punch procedure across all brains. From each brain, the first rostral-most slab from where the corpus callosum first joins the hemispheres was chosen for tissue collection, and the puncher was positioned immediately adjacent to the fundus of the principal sulcus, aligned to an imaginary line connecting the fundi of the principal and cingulate gyrus (Figure 1). Brain biopsies were collected from either the left or the right hemisphere in a random fashion, in two batches. For each monkey a white matter and an adjacent gray matter biopsy were taken from the location described above, with cases and controls from the same batch processed in parallel. The weight of punched gray matter tissue was 33.5 ± 4.5 mg (mean ± S.E.M.), and 31.0 ± 4.7 mg for punches from white matter, with minimal and non-significant differences across treatment groups (−3 % for clozapine and −1 % for haloperidol, in comparison to controls). To prepare for flow cytometry (nuclei extraction, NeuN immunotagging, DAPI staining) and downstream procedures (RNA extraction, purification, rtPCR) frozen brain tissue specimens were powdered with a pestle and mortar on liquid nitrogen, resuspended in 4 ml of ice-cold lysis buffer (0.32 M sucrose, 5 mM CaCl2, 3 mM Mg acetate, 0.1 mM EDTA, 10 mM Tris-HCl pH 8.0) and homogenized by Polytron, using 5 bursts of 5 seconds each, resulting in the destruction of the cell membranes and extraction of nuclei and other cellular organelles. The homogenate was centrifuged (600 g, 10min, 4°C) and the pellet, constituting the crude nuclei fraction, was resuspended in 0.75 ml of Blocking Buffer (1 % goat serum (Jackson Immunoresearch), 2 mM MgCl2, 25 mM Tris, 150 mM NaCl, pH 8). Anti-NeuN antibodies, directly conjugated to Alexa488 fluorophore (Millipore, MAB377X) were added to 1:1000 dilution, and the nuclei were incubated on ice for 1 hour, with occasional swirling. After incubation, the solution was diluted to a volume of 4ml with low concentration sucrose solution (0.35 M sucrose, 3 mM MgCl2, 10 mM Tris-HCl at pH 8). This dilution was then underlaid with a 4ml layer of high concentration sucrose solution (1.1M sucrose, 3 mM MgCl2, 10 mM Tris-HCl at pH 8). Centrifugation followed (2,800g, 20min), the supernatant was removed, and the pellet resuspended in 500μl of a nuclei storage solution (150 mM NaCl, 2 mM MgCl2, 25 mM Tris at pH 8), Lastly, the DNA dye 7-Aminoactinomycin D (7-AAD, Sigma) was added to a final concentration of 2 μg/ml. The resulting nuclei suspension was processed by flow cytometry, including an additional gating step based on the 7-AAD signal intensity, to allow for efficient removal of debris and dividing cells

For quality control, small aliquots of nuclei suspension were examined under a light microscope to verify the extraction and purification of nuclei. To estimate the ‘survival’ of nuclei passing through the flow cytometer, we took 10uL aliquots from the nuclei suspension pior to the FACS procedure, added Trypan blue to stain nuclei and DPBS (Dulbecco’s phosphate buffered saline) to achieve a 10 fold dilution, of which 10 uL were loaded on a hemocytometer (Bright-Line™ Counting Chamber, Hausser Scientific, Horsham, PA). Comparison of hemocytometer- and flow cytometry-based counts (N=8 samples) consistently showed nuclei recovery rates of (mean±S.E.M) 94±9 % by FACS, which is in good agreement with other reports on flow cytometry-based quantification of nuclei from primate brain(Young et al., 2012).

Oligodendrocyte numbers were determined with manual counting limited to white matter tissue punches. To this end, the nuclei pellets were resuspended in PBS, washed and co-incubated overnight at 4°C with two primary antibodies (mouse anti-NeuN, Millipore

MAB#377, 1:1000; rabbit anti-Olig2, Millipore AB9610, 1:2000). The next day the nuclei were washed and then incubated with secondary antibodies (goat anti-mouse Alexa 488 and donkey anti-rabbit Alexa 594, Invitrogen). Nuclei were washed, spread onto glass slides, and counterstained with DAPI. $NeuN^+$, $Olig2^+$, and $DAPI^+$ nuclei were counted in at least 10 fields using a 20× objective. However, due to the very low proportion (< 1% of total nuclei) of $NeuN^+$ nuclei in white matter, sample-to-sample variability for this marker was much higher in manual counts, which had been limited to a total of only 130–200 counted nuclei (oligodendrocytes and neurons) per white matter sample. In contrast, FACS-based nuclei sorting allowed for sample counts capturing on average 250,000 nuclei per sample.

Immunohistochemistry

Prefrontal tissue sections from a naive adult rhesus monkey were processed for immunohistochemistry with NeuN (Millipore, 1:1,000) and Olig2 (Abcam, 1:2,000) antibodies, in conjunction with Alexa Fluor 488 goat anti-rabbit and Alexa Fluor 594 goat anti-mouse IgGs (Invitrogen), using standard procedures. In a second, independent set of immunohistochemistry experiments, small tissue blocks (surface area <0.25 cm^2) were dissected from the dorsolateral prefrontal cortex (Area9/46), immersion-fixed in 4 % paraformaldehyde solution for 15–18 hours, dehydrated in 70 %, 90 % and 100 % ethanol (3 × 30 min each) followed by xylene immersion (3 × 20 min) and paraffin-embedded using a Tissue TEK embedding center. Paraffin embedded tissue blocks were cut in 8 μm thick sections and mounted on slides for immunohistochemistry. Sections of three clozapine-exposed animals with elevated proportions of $NeuN^+$ nuclei in white matter were de-paraffinized using xylazine and ethanol. The sections were rehydrated with water, permeabilized with 0.1 % Triton X-100, followed by NeuN staining (1:100, ABN78A4, EMD Millipore). After mounting the tissue with DAPI Fluoromount-G (0100-200, SouthernBiotech), images of $NeuN^+$ subcortical white matter neurons were taken using a Carl Zeiss CLSM780 microscope. Image processing was done with ImageJ (NIH).

Intranuclear RNA extraction, cDNA conversion and qPCR

From 12 animals (5 control, 4 clozapine, 3 haloperidol), sorted nuclei were available for gene expression studies. Sorted samples were treated with the Arcturus PicoPure RNA Isolation Kit (Applied Biosystems, Cat# 12204-01). Extracted RNA underwent RNase-free DNase treatment (Qiagen), washed, and converted into cDNA using SuperScript VILO MasterMix (Invitrogen), followed by pre-amplification with SsoAdvanced PreAmp Supermix kit according to the manufacturer's instructions. See Supplemental Table 1 for a list of primers and sequences. Real-time PCR was performed using the same set of primers and Power SYBR Green PCR Master Mix (Applied Biosystems) under standard conditions, and cycle thresholds for each of the two genes of interest (*RNA BINDING PROTEIN FOX-1 HOMOLOG 3 = RBFOX3; ATP-BINDING CASSETTE 2 = ABCA2*) subtracted by the averaged cycle threshold of four genes: *GADPH, MBP, SYN1* (*RBFOX3* for *ABCA2* quantification, and vice versa).

RNA-seq (human) RNA was extracted from ~75 mg of gray and white matter dissected from two adult human PFC specimens with no known neurological or psychiatric disease, using Rneasy Lipid Tissue mini kit (catalog #74804, QIAGEN), treated with DNase I, purified,

and diluted to 20 ng/μl. Sequencing libraries were prepared according to the NuGen Ovation RNASeq version 2 protocol, and run on the paired-end 50 bp module in Illumina HiSeq 2000 (Eurofins MWG; Operon). RNA-seq raw reads that passed the QC metric, which is referred to as the "chastity filter" by Illumina, were aligned to the UCSC Homo sapiens reference genome build 19 using the STAR aligner(Dobin et al., 2013), and were visualized using IGV Integrative Genome Viewer(Thorvaldsdottir et al., 2013).

Statistical Analysis

Comparison of the proportion of $NeuN^+$ neuronal nuclei (defined here as the ratio of $NeuN^+$ nuclei to 7-AAD^+ nuclei) across the three treatment groups (control, haloperidol and clozapine) was performed using one-way analyses of covariance (ANCOVA). Age, sex and weight increase during treatment period were included as covariates. The abundance of gene transcripts (*RBFOX3* and *ABCA2*) was examined by separate 3 × 4 ANOVA (treatment groups by compartment [$NeuN^+$ vs. $NeuN^-$ nuclei in white or gray matter]. Significant findings were followed up with Bonferroni corrections. Homogeneity of variance was examined using the Levene's test.

Results

Monkeys were subjected to in vivo neuroimaging at two different time points before and then again 5.5 months after begin of antipsychotic treatment, prior to brain harvest and tissue biopsy for flow cytometry-based neuronal and non-neuronal quantification and, for a subset of brains, cell-type specific RNA analysis (Figure 1). The daily haloperidol dose (4 mg/kg/day) resulted in plasma steady state trough levels approaching 2 ng/ml (Table 1). In patients with schizophrenia, trough levels as low as 0.86 ng/ml have been reported to be therapeutically effective(Nyberg et al., 1995). Furthermore, as expected for D_2-antagonist antipsychotic drugs (Seeman, 2002), haloperidol-treated monkeys showed a 15-fold increase in serum prolactin levels (Table 1). We choose a clozapine dose (5.2 mg/kg/day) that, in multiple independent studies, has been shown to trigger robust shifts in dopamine and NMDA receptor expression and ligand binding in monkey cerebral cortex (see Supplemental Table 2). Of note, this clozapine dose resulted in steady state trough levels of approximately 50 ng/ml (Table 1). While the clinical response in patients does not display a strong correlation with clozapine dose, serum levels of 50 ng/ml would be expected to represent the lower end of therapeutically effective levels defined as preventing psychosis relapse (Ulrich et al., 2003). Some studies suggest that levels around 350 ng/ml increase the probability of a stable antipsychotic effect (Mauri et al., 2007). For each of the 3 treatment groups, the average body weight increased during the trial period (vehicle ~ 1.4 kg; haloperidol, ~ 0.8 kg; clozapine, ~ 1.3 kg (Table 1).

Cell-type composition of antipsychotic-drug-exposed prefrontal white and gray matter

Flow cytometry based assessments of numbers and proportion of cell nuclei prepared from brain homogenate are considered an attractive alternative to conventional stereology, particular in circumstances where the cell type-of-interest is distributed in non-homogenous fashion and at comparatively low frequency(Benes and Lange, 2001; Collins et al., 2010; Hayashi et al., 2012; Herculano-Houzel et al., 2015; Young et al., 2012). These conditions

also apply to subcortical white matter neurons, which show a rapid decline in densities with increasing distance from overlying gray matter and overall comprise far less than 1% of the local cell population in adulthood(Judaš et al., 2010; Kostovic and Rakic, 1980). For all 26 animals included in this study, tissue punches, ~ 30 mg were collected from the superficial white matter bordering the PFC on the dorsolateral convexity and the overlying gray matter (Figure 1). Cell nuclei were purified and immunotagged with neuronal NeuN antibody, which allows for separate counting and collection of (neuronal) $NeuN^+$ and (glial and other non-neuronal) $NeuN^-$ nuclei (Figure 2A–E). This approach is increasingly used to rapidly quantify numbers of neuronal and non-neuronal nuclei in mammalian brains(Herculano-Houzel et al., 2015; Spoelgen et al., 2011), and bypasses many of the limitations associated with two- and three-dimensional cell counting techniques in histological material which face inherent limitations particularly for sparsely occurring cell populations such as the WMN(Benes and Lange, 2001; Herculano-Houzel et al., 2015). The three treatment groups did not differ significantly in the total number of white matter nuclei sorted. We note that clozapine-treated animals showed, on average, a non-significant, ~10–15% decrease in total number of nuclei sorted, in comparison to controls (Mean ± SEM: controls 255,228 ± 91,799; haloperidol, 245,486 ± 87,077; clozapine, 213,861 ± 72,316). In all three treatment groups, the proportion of $NeuN^+$ neuronal nuclei - defined here as the ratio of $NeuN^+$ nuclei to $7\text{-}AAD^+$ nuclei - in the subcortical white matter bordering the six-layered cortex was ~100-fold lower as compared to the overlying gray matter (Figure 2F,G). However, there was an increased proportion of white matter $NeuN^+$ nuclei that reached the level of significance specifically in the clozapine cohort, with an approximately 50% increase when compared to vehicle-treated controls (Figure 2F,G: ANCOVA with sex, age, weight increase during treatment period as covariates, $F_{(2,20)} = 4.296$, main effect $P = 0.028$, Bonferroni-corrected post hoc clozapine > controls, $P = 0.027$. Furthermore, for N = 5 vehicle- and N = 4 clozapine-treated animals, nuclei counts were conducted both in gray and white matter punches, revealing a significant correlation of $NeuN^+$ proportions across gray and white matter (Figure 2H: $R^2 = 0.52$, $P < 0.05$). There were no significant differences in white matter $NeuN^+$ numbers and proportions between haloperidol and control groups (Figure 2F).

Next, we examined whether the clozapine induced increase in white matter neuronal densities is cell-type specific. We first confirmed in macaque brain, processed by perfusion-fixation for conventional histology, the non-overlapping distribution of the $NeuN^+$ population with OLIG2, a transcription factor expressed in a substantial portion of oligodendrocytes (Yokoo et al., 2004)(Figure 2A–D). This finding is in agreement with a recent flow cytometry-based report on (human) brain nuclei(Hayashi et al., 2012). We then prepared from 14 animals (N = 5 CLZ, 5 CTRL, 4 HAL) from a second round of subcortical white matter punches nuclei spreads on glass slides for OLIG2 immunostaining, counterstained with the nucleophilic dye DAPI (4',6-Diamidino-2-Phenylindole, Dihydrochloride). Because the proportion of white matter $OLIG2^+$ nuclei is up to two order of magnitude higher in comparison to white mater $NeuN^+$ nuclei (Figure 2F,I), FACS-based quantification for this type of non-neuronal nuclei was less critical and instead we manually counted the proportion of $OLIG2^+$ nuclei, expressed as % of $DAPI^+$ nuclei. Approximately 70% from the total pool of counted nuclei were $OLIG2^+$, and no significant differences between antipsychotic drug and vehicle groups emerged (Figure 2I). Due to the very low

proportion of $NeuN^+$ nuclei in white matter, we could not reliably quantify this subpopulation by our manual counts with 130–200 nuclei as input/sample. Because antipsychotic drugs did not affect the proportion of $OLIG2^+$ nuclei (Figure 2I), the aforementioned alterations in $NeuN^+$ nuclei numbers of the clozapine-exposed monkeys are specific for that cell population. To evaluate the potential confound of brain volume differences, we conducted *in vivo* structural neuroimaging at two time points for a subset of 17 monkeys (Table 1). To this end, gray and white matter volumes were determined for the dorso- and medio-lateral portions of the frontal lobe at multiple time points (before and towards the end of treatment, Figure 1), with clozapine- (N=5) and haloperidol-treated (N=7) monkeys essentially indistinguishable from controls (N=5) (Figure 3). There were no significant group effects or interactions (all $P > 0.4$) by MANOVA 2 × 2, (Gray/White matter × Pre-/Post-treatment). As additional control (to rule out effect by side), all measurements were repeated with the left hemisphere masked, further confirming that differences in frontal lobe volumes were minimal and non-significant across all three groups (Supplemental Figure 1). Taken together, these multiple lines of evidence strongly argue against the possibility that volumetric changes contributed to the significantly increased proportion of white matter $NeuN^+$ nuclei in the clozapine-treated animals.

Next, we examined whether the molecular 'fingerprint' of $NeuN^+$ nuclei is altered after clozapine exposure, by measuring the expression of *RBFOX3* encoding the neuron-specific NeuN protein, and *ABCA2* (*ATP Binding Cassette 2*), a gene predominantly expressed by white matter oligodendrocytes (Zhou et al., 2001). Tissue from 12 of the 26 monkeys included in this study was available for RNA analysis (Table 1). Given that macaque tissues show very high degrees (92–95%) of transcriptome conservation in comparison to human(Peng et al., 2015), we wanted to study in our monkey specimens a set of transcripts subject to differential expression in human gray and white matter. To this end, we analyzed our RNAseq datasets from human postmortem gray and white matter homogenates(Dincer et al., 2015), and confirmed that the *RBFOX3* and *ABCA2* transcripts show strikingly different distribution. Thus, *RBFOX3* showed, as expected, strong expression in the (neuron-rich) gray matter, while *ABCA2* expression was much higher in (oligodendrocyte-rich) white matter (Supplemental Figure 2). To avoid *RBFOX3* RNA signal from axons or fibers of passage crossing through the white matter, we next extracted RNA from sorted $NeuN^+$ and $NeuN^-$ nuclei from the gray and white matter of 4 clozapine monkeys, and compared these to 5 vehicle-treated and 3 haloperidol exposed animals. The RNA quantification from monkey nuclei resonated with the human gray and white matter RNA-seq. Thus, *RBFOX3* was expressed at much higher levels in $NeuN^+$ as compared to $NeuN^-$ nuclei, independent of treatment (Figure 4A). The abundance of *RBFOX3* and *ABCA2* transcripts was compared by 3 × 2 × 2 ANOVA, (treatment [control vs. haloperidol vs. clozapine] × compartment [$NeuN^+$ vs. $NeuN^-$ nuclei] in white or gray matter. A significant effect of compartment was found for *RBFOX3:* $F_{(3,36)} = 7.668$, $P = 0.0004$, Bonferroni-corrected post hoc $NeuN^+$ in gray matter > $NeuN^-$ in gray matter, $P = 0.001$ or $NeuN^-$ in white matter, $P = 0.011$. Similarly, a significant effect of compartment was found for *ABCA2*: $F_{(3,36)} = 7.118$, $P = 0.001$, Bonferroni-corrected post hoc $NeuN^-$ in white matter > $NeuN^-$ in gray matter, $P = 0.006$ or $NeuN^+$ in gray matter, $P = 0.001$. However, for both transcripts, there was no significant effect by treatment (Figure 4A). Furthermore, in sharp contrast to this cell-type

specific *ABCA2* expression in white matter, expression of this gene in gray matter was slightly higher in gray matter NeuN$^+$ nuclei as compared to gray matter NeuN$^-$ nuclei, but again no significant effects by treatment were observed (Figure 4B). Taken together, our RNA studies suggest that NeuN$^+$ nuclei show a differential RNA expression pattern from NeuN$^-$, but these cell type-specific molecular fingerprints were not altered after clozapine and haloperidol treatment (Figure 4B). We conclude that neuronal gene expression patterns are maintained in white matter NeuN$^+$ nuclei exposed to antipsychotic drug treatment (including clozapine). To further confirm the neuronal phenotype of NeuN immunoreactive white matter nuclei, we performed NeuN immunohistochemistry/DAPI counterstain on immersion-fixed, paraffin-embedded tissue blocks from the ventrolateral PFC of N=3 clozapine-treated animals with elevated white matter neuron densities. Remarkably, when examining white matter NeuN$^+$ nuclei under the microscope, 150/150 nuclei counted bear hallmarks characteristic for neuronal nuclei, including a prominent nucleolus with heterochromatic shell(Akbarian et al., 2001; Akhmanova et al., 2000; Thatcher and LaSalle, 2006) and/or a decondensed chromatin with overall much less compacted (hetero-)chromatin as compared to the surrounding non-neuronal (NeuN$^-$) nuclei (subset of 3 monkeys, 50 white matter nuclei counted per monkey with a minimum diameter of 8 μm, see Supplemental Figure 3).

Discussion

In this non-human primate study, clozapine exposure was associated with a significantly (~ 50%) increased proportion of NeuN$^+$ nuclei in frontal subcortical white matter. This was correlated with a much milder elevation of NeuN$^+$ proportions in the overlying gray matter, which could reflect common regulatory mechanisms across the two anatomical compartments. These alterations were highly specific, because OLIG2$^+$ nuclei, representing the oligodendrocyte lineage(Yokoo et al., 2004) and in complete non-overlap with the NeuN + population (Figure 1A–D), remained unaffected after clozapine treatment. Furthermore, haloperidol in contrast to clozapine elicited only a mild, non-significant increase in the proportion of white matter NeuN+ nuclei, and frontal lobe volumes were unaffected by antipsychotic drug treatment.

It is also noteworthy that while the haloperidol-treated monkeys of the present study showed a mild increase in proportions of NeuN$^+$ nuclei, these changes—in contrast to those in the clozapine-treated animals—did not reach the level of significance (Figure 2F,G). However, we cannot exclude a more robust haloperidol-mediated effect if treatment would have continued beyond 6 months. The findings reported here could explain the long-standing observation on increased numbers and densities of white matter neurons in cases diagnosed with schizophrenia (reviewed in (Connor et al., 2011)). The underlying etiologies for these histological phenotypes are often discussed in the context of neurodevelopment (Anderson et al., 1996; Eastwood and Harrison, 2005; Kanold, 2004; Kostovic et al., 2011; Rioux et al., 2003). However, in light of the present study, medication effects are very likely to contribute. Adult white matter neurons remain functionally interconnected with the overlying cortex (Torres-Reveron and Friedlander, 2007) therefore clozapine-mediated changes in cell composition in white matter could lead to a partial rewiring of prefrontal circuitry. Given the drug's superior efficacy in comparison to other antipsychotic drugs

(Miyamoto et al., 2012), further exploration the mechanisms underlying drug-induced plasticity in cell composition could reveal important insights into novel therapeutic mechanisms.

What types of cellular and molecular mechanisms could lead to altered cell composition and phenotypic marker expression in the antipsychotic-drug-exposed monkeys? The most parsimonious explanation would be subtle changes in expression of the phenotypic marker NeuN, reflecting increased proportion of $NeuN^+$ nuclei, independent of any concurrent loss of glia. Increased NeuN expression in a subset of WMN and other neurons in clozapine-exposed monkey brain would not require generation of new neurons, which at baseline is unlikely to occur in primate neocortex(Kornack and Rakic, 2001). Notably, subcortical white matter of the adult human frontal lobe harbors a sparse cell population bearing morphological and neurochemical hallmarks that define young, immature neurons (Fung et al., 2011). Therefore, it is possible that the findings of the present study (incl. the overwhelming, if not exclusive neuronal phenotype of NeuN+ white matter nuclei in clozapine-exposed animals) are best explained by a surprising degree of phenotypic plasticity, as evidenced by increased expression and detectability of the NeuN immunoreactive marker. Phenotyic plasticity after antipsychotic drug exposure has previously reported for the rodent brain, including reduced cortical volumes and elevated astrocyte densities (Barr et al., 2013; Vernon et al., 2014; Vernon et al., 2012; Vernon et al., 2011). Furthermore, antipsychotic drugs trigger proliferative activity in the proliferative layers of the rodent subventricular zone (Nasrallah et al., 2010; Wang et al., 2004), and may promote hippocampal neurogenesis(Peng et al., 2013), suggesting that additional brain regions other than the subcortical white matter may also show altered proportion of neurons in antipsychotic-exposed monkey brain, Additional factors that could contribute to the observed increase in NeuN+ nuclei after antipsychotic drug treatment could include subtle losses of non-neuronal cells, including a subset of astrocytes or oligodendroglia as previously suggested (Dorph-Petersen et al., 2005; Konopaske et al., 2007; Konopaske et al., 2008). Additional studies are required to gain deeper insights into antipsychotic-induced changes in cell compositions in the non-human primate brain. In this context, it is noteworthy that the total number of sorted nuclei from our tissue punches was 15% and 8% lower in the clozapine and haloperidol animals as compared to control monkeys (see *Results*), albeit these differences did not reach the level of significance. Furthermore, our flow cytometry-based quantifications, while informing about proportion of (cell) nuclei types, do not allow solid conclusion about potential changes in in absolute number of cells (which would require processing and counting entire cortical hemispheres). Nonetheless, taken together with the increase in the proportion of $NeuN^+$ white matter nuclei, particularly in the clozapine group, a net loss of non-neuronal cells therefore appears plausible. According to previous work, this effects is expected to be driven primarily by a decrease in numbers of astrocytes and additional deficits in oligodendroglia (Konopaske et al., 2008), a cell type broadly affected in many cases with schizophrenia (Hoistad et al., 2009). Finally, it is important to further discuss some of the limitations of the current study, including the antipsychotic treatment period which was limited to 5.5 months and did not result in detectable changes in frontal lobe volumes, which contrasts with previous reports in animals treated up to 27 months with antipsychotics, which resulted in mild, ~8–15% reductions in

brain weight and regional volumes (Dorph-Petersen et al., 2005; Konopaske et al., 2007; Konopaske et al., 2008). Differential effects on brain (incl. cerebral cortex) volumes have been previously reported in rodents in which the duration of antipsychotic treatment varied from 1 to 2 months(Vernon et al., 2011) and in large cohorts of patients with schizophrenia(Haijma et al., 2013). On the other hand, evidence is emerging that gray matter loss in schizophrenia reflects the underlying disease process irrespective of clozapine treatment(Ahmed et al., 2015; Anderson et al., 2015). Therefore, the lack of frontal lobe volume changes in the clozapine-treated monkeys of the present study could also be explained, in part, by the absence of the underlying disease process (schizophrenia) in the animals.

Our results strongly suggest that clozapine-induced changes in cell type-specific phenotypic marker expression could occur independently of, or at least prior to any ensuing losses in brain regional volumes or tissue mass. Finally, as mentioned already above, the findings presented here warrant at least a partial reinterpretation of the reported supernormal WMN numbers and densities in prefrontal, cingulate and medial or lateral temporal cortex of subjects diagnosed with schizophrenia(Akbarian et al., 1993a; Akbarian et al., 1996; Akbarian et al., 1993b; Anderson et al., 1996; Eastwood and Harrison, 2003, 2005; Ikeda et al., 2004; Joshi et al., 2012; Kirkpatrick et al., 1999; Kirkpatrick et al., 2003; Rioux et al., 2003; Yang et al., 2011). These alterations, which may be more prominent in subjects diagnosed with deficit syndrome and negative symptoms(Kirkpatrick et al., 2003), have been hitherto primarily interpretated as evidence for defective neurodevelopment(Kostovic et al., 2011). Given that the NeuN (also known as RBFOX3) protein broadly regulates microRNA biogenesis(Kim et al., 2014) and alternative splicing(Dredge and Jensen, 2011; Gehman et al., 2012; Kim et al., 2013) in the neuronal transcriptome, further studies, using larger cohorts, are necessary to evaluate the functional (including therapeutic) impact of this clozapine-mediated effect of specific neuronal subpopulations (including WMN) of the human and non-human primate brain.

Supplementary Material

Refer to Web version on PubMed Central for supplementary material.

Acknowledgments

The authors thank Brian Horman, Jim Daunais, Yin Guo, Lily C. Lin, and the staff from the Wake Forest University Primate Center for excellent technical support.

Funding:

This study was supported by grants from the Brain Behavior Research Foundation, National Institutes of Health grant R01MH093332, MH074313 and Stanley Medical Research Institute.

References

Ahmed M, Cannon DM, Scanlon C, Holleran L, Schmidt H, McFarland J, Langan C, McCarthy P, Barker GJ, Hallahan B, McDonald C. Progressive Brain Atrophy and Cortical Thinning in Schizophrenia after Commencing Clozapine Treatment. Neuropsychopharmacology : official publication of the American College of Neuropsychopharmacology. 2015

Akbarian S, Bunney WE Jr, Potkin SG, Wigal SB, Hagman JO, Sandman CA, Jones EG. Altered distribution of nicotinamide-adenine dinucleotide phosphate-diaphorase cells in frontal lobe of schizophrenics implies disturbances of cortical development. Arch Gen Psychiatry. 1993a; 50(3): 169–177. [PubMed: 7679891]

Akbarian S, Chen RZ, Gribnau J, Rasmussen TP, Fong H, Jaenisch R, Jones EG. Expression pattern of the Rett syndrome gene MeCP2 in primate prefrontal cortex. Neurobiol Dis. 2001; 8(5):784–791. [PubMed: 11592848]

Akbarian S, Kim JJ, Potkin SG, Hetrick WP, Bunney WE Jr, Jones EG. Maldistribution of interstitial neurons in prefrontal white matter of the brains of schizophrenic patients. Arch Gen Psychiatry. 1996; 53(5):425–436. [PubMed: 8624186]

Akbarian S, Vinuela A, Kim JJ, Potkin SG, Bunney WE Jr, Jones EG. Distorted distribution of nicotinamide-adenine dinucleotide phosphate-diaphorase neurons in temporal lobe of schizophrenics implies anomalous cortical development. Arch Gen Psychiatry. 1993b; 50(3):178–187. [PubMed: 7679892]

Akhmanova A, Verkerk T, Langeveld A, Grosveld F, Galjart N. Characterisation of transcriptionally active and inactive chromatin domains in neurons. J Cell Sci. 2000; 113(Pt 24):4463–4474. [PubMed: 11082040]

Anderson SA, Volk DW, Lewis DA. Increased density of microtubule associated protein 2-immunoreactive neurons in the prefrontal white matter of schizophrenic subjects. Schizophrenia research. 1996; 19(2–3):111–119. [PubMed: 8789909]

Anderson VM, Goldstein ME, Kydd RR, Russell BR. Extensive gray matter volume reduction in treatment-resistant schizophrenia. Int J Neuropsychopharmacol. 2015; 18(7):pyv016. [PubMed: 25716781]

Barr AM, Wu CH, Wong C, Hercher C, Topfer E, Boyda HN, Procyshyn RM, Honer WG, Beasley CL. Effects of chronic exercise and treatment with the antipsychotic drug olanzapine on hippocampal volume in adult female rats. Neuroscience. 2013; 255:147–157. [PubMed: 24141179]

Beasley CL, Cotter DR, Everall IP. Density and distribution of white matter neurons in schizophrenia, bipolar disorder and major depressive disorder: no evidence for abnormalities of neuronal migration. Molecular psychiatry. 2002; 7(6):564–570. [PubMed: 12140779]

Beasley CL, Honavar M, Everall IP, Cotter D. Two-dimensional assessment of cytoarchitecture in the superior temporal white matter in schizophrenia, major depressive disorder and bipolar disorder. Schizophrenia research. 2009; 115(2–3):156–162. [PubMed: 19833481]

Benes FM, Lange N. Two-dimensional versus three-dimensional cell counting: a practical perspective. Trends in neurosciences. 2001; 24(1):11–17. [PubMed: 11163882]

Collins CE, Young NA, Flaherty DK, Airey DC, Kaas JH. A rapid and reliable method of counting neurons and other cells in brain tissue: a comparison of flow cytometry and manual counting methods. Front Neuroanat. 2010; 4:5. [PubMed: 20300202]

Connor CM, Crawford BC, Akbarian S. White matter neuron alterations in schizophrenia and related disorders. International journal of developmental neuroscience : the official journal of the International Society for Developmental Neuroscience. 2011; 29(3):325–334. [PubMed: 20691252]

Connor CM, Guo Y, Akbarian S. Cingulate white matter neurons in schizophrenia and bipolar disorder. Biological psychiatry. 2009; 66(5):486–493. [PubMed: 19559403]

Dincer A, Gavin DP, Xu K, Zhang B, Dudley JT, Schadt EE, Akbarian S. Deciphering H3K4me3 broad domains associated with gene-regulatory networks and conserved epigenomic landscapes in the human brain. Transl Psychiatry. 2015; 5:e679. [PubMed: 26575220]

Dobin A, Davis CA, Schlesinger F, Drenkow J, Zaleski C, Jha S, Batut P, Chaisson M, Gingeras TR. STAR: ultrafast universal RNA-seq aligner. Bioinformatics. 2013; 29(1):15–21. [PubMed: 23104886]

Dorph-Petersen KA, Pierri JN, Perel JM, Sun Z, Sampson AR, Lewis DA. The influence of chronic exposure to antipsychotic medications on brain size before and after tissue fixation: a comparison of haloperidol and olanzapine in macaque monkeys. Neuropsychopharmacology : official publication of the American College of Neuropsychopharmacology. 2005; 30(9):1649–1661. [PubMed: 15756305]

Dredge BK, Jensen KB. NeuN/Rbfox3 nuclear and cytoplasmic isoforms differentially regulate alternative splicing and nonsense-mediated decay of Rbfox2. PloS one. 2011; 6(6):e21585. [PubMed: 21747913]

Eastwood SL, Harrison PJ. Interstitial white matter neurons express less reelin and are abnormally distributed in schizophrenia: towards an integration of molecular and morphologic aspects of the neurodevelopmental hypothesis. Molecular psychiatry. 2003; 8(9):769, 821–731. [PubMed: 12931209]

Eastwood SL, Harrison PJ. Interstitial white matter neuron density in the dorsolateral prefrontal cortex and parahippocampal gyrus in schizophrenia. Schizophrenia research. 2005; 79(2–3):181–188. [PubMed: 16076548]

Feher LZ, Kalman J, Puskas LG, Gyulveszi G, Kitajka K, Penke B, Palotas M, Samarova EI, Molnar J, Zvara A, Matin K, Bodi N, Hugyecz M, Pakaski M, Bjelik A, Juhasz A, Bogats G, Janka Z, Palotas A. Impact of haloperidol and risperidone on gene expression profile in the rat cortex. Neurochemistry international. 2005; 47(4):271–280. [PubMed: 15941608]

Fung SJ, Joshi D, Allen KM, Sivagnanasundaram S, Rothmond DA, Saunders R, Noble PL, Webster MJ, Weickert CS. Developmental patterns of doublecortin expression and white matter neuron density in the postnatal primate prefrontal cortex and schizophrenia. PloS one. 2011; 6(9):e25194. [PubMed: 21966452]

Gehman LT, Meera P, Stoilov P, Shiue L, O'Brien JE, Meisler MH, Ares M Jr, Otis TS, Black DL. The splicing regulator Rbfox2 is required for both cerebellar development and mature motor function. Genes & development. 2012; 26(5):445–460. [PubMed: 22357600]

Girgenti MJ, Nisenbaum LK, Bymaster F, Terwilliger R, Duman RS, Newton SS. Antipsychotic-induced gene regulation in multiple brain regions. Journal of neurochemistry. 2010; 113(1):175–187. [PubMed: 20070867]

Haijma SV, Van Haren N, Cahn W, Koolschijn PC, Hulshoff Pol HE, Kahn RS. Brain volumes in schizophrenia: a meta-analysis in over 18 000 subjects. Schizophr Bull. 2013; 39(5):1129–1138. [PubMed: 23042112]

Hayashi Y, Nihonmatsu-Kikuchi N, Hisanaga S, Yu XJ, Tatebayashi Y. Neuropathological similarities and differences between schizophrenia and bipolar disorder: a flow cytometric postmortem brain study. PloS one. 2012; 7(3):e33019. [PubMed: 22438888]

Herculano-Houzel S, von Bartheld CS, Miller DJ, Kaas JH. How to count cells: the advantages and disadvantages of the isotropic fractionator compared with stereology. Cell and tissue research. 2015; 360(1):29–42. [PubMed: 25740200]

Hoistad M, Segal D, Takahashi N, Sakurai T, Buxbaum JD, Hof PR. Linking white and grey matter in schizophrenia: oligodendrocyte and neuron pathology in the prefrontal cortex. Frontiers in neuroanatomy. 2009; 3:9. [PubMed: 19636386]

Iancu OD, Darakjian P, Malmanger B, Walter NA, McWeeney S, Hitzemann R. Gene networks and haloperidol-induced catalepsy. Genes, brain, and behavior. 2012; 11(1):29–37.

Ikeda K, Ikeda K, Iritani S, Ueno H, Niizato K. Distribution of neuropeptide Y interneurons in the dorsal prefrontal cortex of schizophrenia. Progress in neuropsychopharmacology & biological psychiatry. 2004; 28(2):379–383.

Ji B, Zhang Z, Zhang M, Zhu H, Zhou K, Yang J, Li Y, Sun L, Feng G, Wang Y, He L, Wan C. Differential expression profiling of the synaptosome proteome in a rat model of antipsychotic resistance. Brain research. 2009; 1295:170–178. [PubMed: 19660441]

Joshi D, Fung SJ, Rothwell A, Weickert CS. Higher gamma-aminobutyric acid neuron density in the white matter of orbital frontal cortex in schizophrenia. Biological psychiatry. 2012; 72(9):725–733. [PubMed: 22841514]

Judaš M, Sedmak G, Pletikos M, Jovanov-Milošević N. Populations of subplate and interstitial neurons in fetal and adult human telencephalon. J Anat. 2010; 217(4):381–399. [PubMed: 20979586]

Kanold PO. Transient microcircuits formed by subplate neurons and their role in functional development of thalamocortical connections. Neuroreport. 2004; 15(14):2149–2153. [PubMed: 15371723]

Kim KK, Nam J, Mukouyama YS, Kawamoto S. Rbfox3-regulated alternative splicing of Numb promotes neuronal differentiation during development. The Journal of cell biology. 2013; 200(4): 443–458. [PubMed: 23420872]

Kim KK, Yang Y, Zhu J, Adelstein RS, Kawamoto S. Rbfox3 controls the biogenesis of a subset of microRNAs. Nature structural & molecular biology. 2014; 21(10):901–910.

Kirkpatrick B, Conley RC, Kakoyannis A, Reep RL, Roberts RC. Interstitial cells of the white matter in the inferior parietal cortex in schizophrenia: An unbiased cell-counting study. Synapse. 1999; 34(2):95–102. [PubMed: 10502308]

Kirkpatrick B, Messias NC, Conley RR, Roberts RC. Interstitial cells of the white matter in the dorsolateral prefrontal cortex in deficit and nondeficit schizophrenia. J Nerv Ment Dis. 2003; 191(9):563–567. [PubMed: 14504564]

Konopaske GT, Dorph-Petersen KA, Pierri JN, Wu Q, Sampson AR, Lewis DA. Effect of chronic exposure to antipsychotic medication on cell numbers in the parietal cortex of macaque monkeys. Neuropsychopharmacology : official publication of the American College of Neuropsychopharmacology. 2007; 32(6):1216–1223. [PubMed: 17063154]

Konopaske GT, Dorph-Petersen KA, Sweet RA, Pierri JN, Zhang W, Sampson AR, Lewis DA. Effect of chronic antipsychotic exposure on astrocyte and oligodendrocyte numbers in macaque monkeys. Biological psychiatry. 2008; 63(8):759–765. [PubMed: 17945195]

Kornack DR, Rakic P. Cell proliferation without neurogenesis in adult primate neocortex. Science. 2001; 294(5549):2127–2130. [PubMed: 11739948]

Kostovic I, Judas M, Sedmak G. Developmental history of the subplate zone, subplate neurons and interstitial white matter neurons: relevance for schizophrenia. Int J Dev Neurosci. 2011; 29(3): 193–205. [PubMed: 20883772]

Kostovic I, Rakic P. Cytology and time of origin of interstitial neurons in the white matter in infant and adult human and monkey telencephalon. J Neurocytol. 1980; 9(2):219–242. [PubMed: 7441294]

Lidow MS, Elsworth JD, Goldman-Rakic PS. Down-regulation of the D1 and D5 dopamine receptors in the primate prefrontal cortex by chronic treatment with antipsychotic drugs. Journal of Pharmacology & Experimental Therapeutics. 1997; 281(1):597–603. [PubMed: 9103549]

Lidow MS, Goldman-Rakic PS. A common action of clozapine, haloperidol, and remoxipride on D1- and D2-dopaminergic receptors in the primate cerebral cortex. Proceedings of the National Academy of Sciences of the United States of America. 1994; 91(10):4353–4356. [PubMed: 8183912]

Lidow MS, Goldman-Rakic PS. Differential regulation of D2 and D4 dopamine receptor mRNAs in the primate cerebral cortex vs. neostriatum: effects of chronic treatment with typical and atypical antipsychotic drugs. Journal of Pharmacology & Experimental Therapeutics. 1997; 283(2):939–946. [PubMed: 9353417]

Lieberman JA, Stroup TS, McEvoy JP, Swartz MS, Rosenheck RA, Perkins DO, Keefe RS, Davis SM, Davis CE, Lebowitz BD, Severe J, Hsiao JK. Effectiveness of antipsychotic drugs in patients with chronic schizophrenia. The New England journal of medicine. 2005; 353(12):1209–1223. [PubMed: 16172203]

Ma D, Chan MK, Lockstone HE, Pietsch SR, Jones DN, Cilia J, Hill MD, Robbins MJ, Benzel IM, Umrania Y, Guest PC, Levin Y, Maycox PR, Bahn S. Antipsychotic treatment alters protein expression associated with presynaptic function and nervous system development in rat frontal cortex. Journal of proteome research. 2009; 8(7):3284–3297. [PubMed: 19400588]

Mauri MC, Volonteri LS, Colasanti A, Fiorentini A, De Gaspari IF, Bareggi SR. Clinical pharmacokinetics of atypical antipsychotics: a critical review of the relationship between plasma concentrations and clinical response. Clinical pharmacokinetics. 2007; 46(5):359–388. [PubMed: 17465637]

Meltzer HY. Update on typical and atypical antipsychotic drugs. Annual review of medicine. 2013; 64:393–406.

Middleton FA, Mirnics K, Pierri JN, Lewis DA, Levitt P. Gene expression profiling reveals alterations of specific metabolic pathways in schizophrenia. The Journal of neuroscience : the official journal of the Society for Neuroscience. 2002; 22(7):2718–2729. [PubMed: 11923437]

Miyamoto S, Miyake N, Jarskog LF, Fleischhacker WW, Lieberman JA. Pharmacological treatment of schizophrenia: a critical review of the pharmacology and clinical effects of current and future therapeutic agents. Molecular psychiatry. 2012; 17(12):1206–1227. [PubMed: 22584864]

Mullen RJ, Buck CR, Smith AM. NeuN, a neuronal specific nuclear protein in vertebrates. Development. 1992; 116(1):201–211. [PubMed: 1483388]

Nasrallah HA, Hopkins T, Pixley SK. Differential effects of antipsychotic and antidepressant drugs on neurogenic regions in rats. Brain Res. 2010; 1354:23–29. [PubMed: 20682307]

Nyberg S, Farde L, Halldin C, Dahl ML, Bertilsson L. D2 dopamine receptor occupancy during low-dose treatment with haloperidol decanoate. The American journal of psychiatry. 1995; 152(2): 173–178. [PubMed: 7840348]

Peng X, Thierry-Mieg J, Thierry-Mieg D, Nishida A, Pipes L, Bozinoski M, Thomas MJ, Kelly S, Weiss JM, Raveendran M, Muzny D, Gibbs RA, Rogers J, Schroth GP, Katze MG, Mason CE. Tissue-specific transcriptome sequencing analysis expands the non-human primate reference transcriptome resource (NHPRTR). Nucleic Acids Res. 2015; 43(Database issue):D737–D742. [PubMed: 25392405]

Peng Z, Zhang R, Wang H, Chen Y, Xue F, Wang L, Yang F, Chen Y, Liu L, Kuang F, Tan Q. Ziprasidone ameliorates anxiety-like behaviors in a rat model of PTSD and up-regulates neurogenesis in the hippocampus and hippocampus-derived neural stem cells. Behav Brain Res. 2013; 244:1–8. [PubMed: 23384713]

Rioux L, Nissanov J, Lauber K, Bilker WB, Arnold SE. Distribution of microtubule-associated protein MAP2-immunoreactive interstitial neurons in the parahippocampal white matter in subjects with schizophrenia. The American journal of psychiatry. 2003; 160(1):149–155. [PubMed: 12505814]

Seeman P. Atypical antipsychotics: mechanism of action. Canadian journal of psychiatry. Revue canadienne de psychiatrie. 2002; 47(1):27–38. [PubMed: 11873706]

Smith SM. Fast robust automated brain extraction. Human brain mapping. 2002; 17(3):143–155. [PubMed: 12391568]

Spoelgen R, Meyer A, Moraru A, Kirsch F, Vogt-Eisele A, Plaas C, Pitzer C, Schneider A. A novel flow cytometry-based technique to measure adult neurogenesis in the brain. Journal of neurochemistry. 2011; 119(1):165–175. [PubMed: 21812782]

Swartz MS, Perkins DO, Stroup TS, Davis SM, Capuano G, Rosenheck RA, Reimherr F, McGee MF, Keefe RS, McEvoy JP, Hsiao JK, Lieberman JA. Effects of antipsychotic medications on psychosocial functioning in patients with chronic schizophrenia: findings from the NIMH CATIE study. The American journal of psychiatry. 2007; 164(3):428–436. [PubMed: 17329467]

Thatcher KN, LaSalle JM. Dynamic changes in Histone H3 lysine 9 acetylation localization patterns during neuronal maturation require MeCP2. Epigenetics. 2006; 1(1):24–31. [PubMed: 17464364]

Thorvaldsdottir H, Robinson JT, Mesirov JP. Integrative Genomics Viewer (IGV): high-performance genomics data visualization and exploration. Briefings in bioinformatics. 2013; 14(2):178–192. [PubMed: 22517427]

Torres-Reveron J, Friedlander MJ. Properties of persistent postnatal cortical subplate neurons. The Journal of neuroscience : the official journal of the Society for Neuroscience. 2007; 27(37):9962–9974. [PubMed: 17855610]

Ulrich S, Baumann B, Wolf R, Lehmann D, Peters B, Bogerts B, Meyer FP. Therapeutic drug monitoring of clozapine and relapse--a retrospective study of routine clinical data. International journal of clinical pharmacology and therapeutics. 2003; 41(1):3–13. [PubMed: 12564740]

Vernon AC, Crum WR, Lerch JP, Chege W, Natesan S, Modo M, Cooper JD, Williams SC, Kapur S. Reduced cortical volume and elevated astrocyte density in rats chronically treated with antipsychotic drugs-linking magnetic resonance imaging findings to cellular pathology. Biological psychiatry. 2014; 75(12):982–990. [PubMed: 24143881]

Vernon AC, Natesan S, Crum WR, Cooper JD, Modo M, Williams SC, Kapur S. Contrasting effects of haloperidol and lithium on rodent brain structure: a magnetic resonance imaging study with postmortem confirmation. Biological psychiatry. 2012; 71(10):855–863. [PubMed: 22244831]

Vernon AC, Natesan S, Modo M, Kapur S. Effect of chronic antipsychotic treatment on brain structure: a serial magnetic resonance imaging study with ex vivo and postmortem confirmation. Biological psychiatry. 2011; 69(10):936–944. [PubMed: 21195390]

Wang HD, Dunnavant FD, Jarman T, Deutch AY. Effects of antipsychotic drugs on neurogenesis in the forebrain of the adult rat. Neuropsychopharmacology. 2004; 29(7):1230–1238. [PubMed: 15085089]

Wenthur CJ, Lindsley CW. Classics in chemical neuroscience: clozapine. ACS chemical neuroscience. 2013; 4(7):1018–1025. [PubMed: 24047509]

Yang Y, Fung SJ, Rothwell A, Tianmei S, Weickert CS. Increased interstitial white matter neuron density in the dorsolateral prefrontal cortex of people with schizophrenia. Biological psychiatry. 2011; 69(1):63–70. [PubMed: 20974464]

Yokoo H, Nobusawa S, Takebayashi H, Ikenaka K, Isoda K, Kamiya M, Sasaki A, Hirato J, Nakazato Y. Anti-human Olig2 antibody as a useful immunohistochemical marker of normal oligodendrocytes and gliomas. The American journal of pathology. 2004; 164(5):1717–1725. [PubMed: 15111318]

Young NA, Flaherty DK, Airey DC, Varlan P, Aworunse F, Kaas JH, Collins CE. Use of flow cytometry for high-throughput cell population estimates in brain tissue. Front Neuroanat. 2012; 6:27. [PubMed: 22798947]

Zhang Y, Brady M, Smith S. Segmentation of brain MR images through a hidden Markov random field model and the expectation-maximization algorithm. IEEE transactions on medical imaging. 2001; 20(1):45–57. [PubMed: 11293691]

Zhou C, Zhao L, Inagaki N, Guan J, Nakajo S, Hirabayashi T, Kikuyama S, Shioda S. Atp-binding cassette transporter ABC2/ABCA2 in the rat brain: a novel mammalian lysosome-associated membrane protein and a specific marker for oligodendrocytes but not for myelin sheaths. The Journal of neuroscience : the official journal of the Society for Neuroscience. 2001; 21(3):849–857. [PubMed: 11157071]

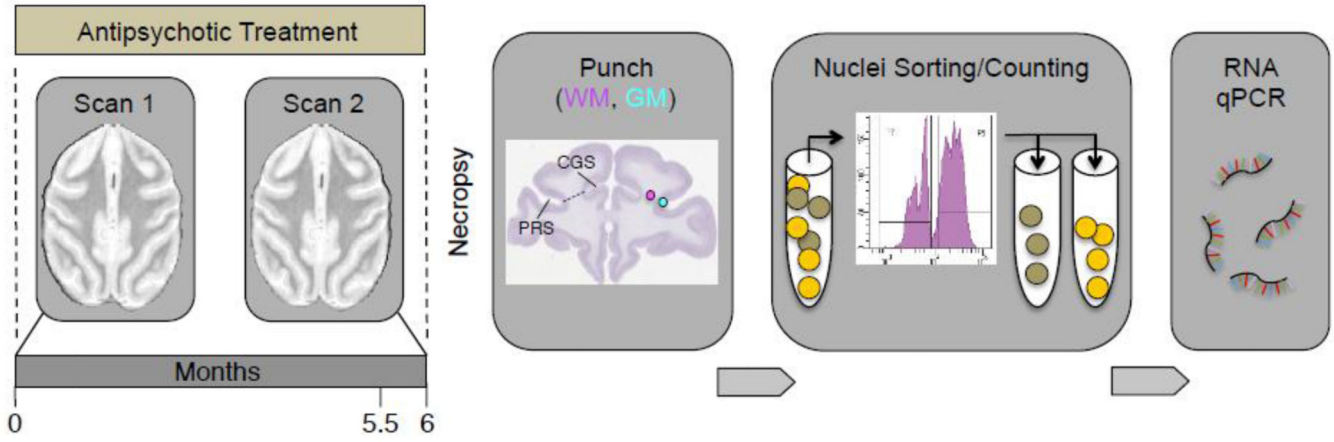

Figure 1. Time line and sequential order of experiments

Monkeys received daily haloperidol and clozapine for 6 months, with in *vivo* neuroimaging (structural MRI) scans first before, and then again at 5.5 months after begin of treatment. After necropsy, punches from frontal subcortical white matter (WM), and from overlying cortex (GM, gray matter), were obtained for extraction and fluorescence-activated sorting, separation and counting of immunotagged nuclei, followed by PCR-based quantification of RNA extracted from sorted cell-type specific ($NeuN^+$ and $NeuN^-$) nuclei. Nissl-stained coronal image from brainmap.org. PRS = principal sulcus, CGS = cingulate sulcus.

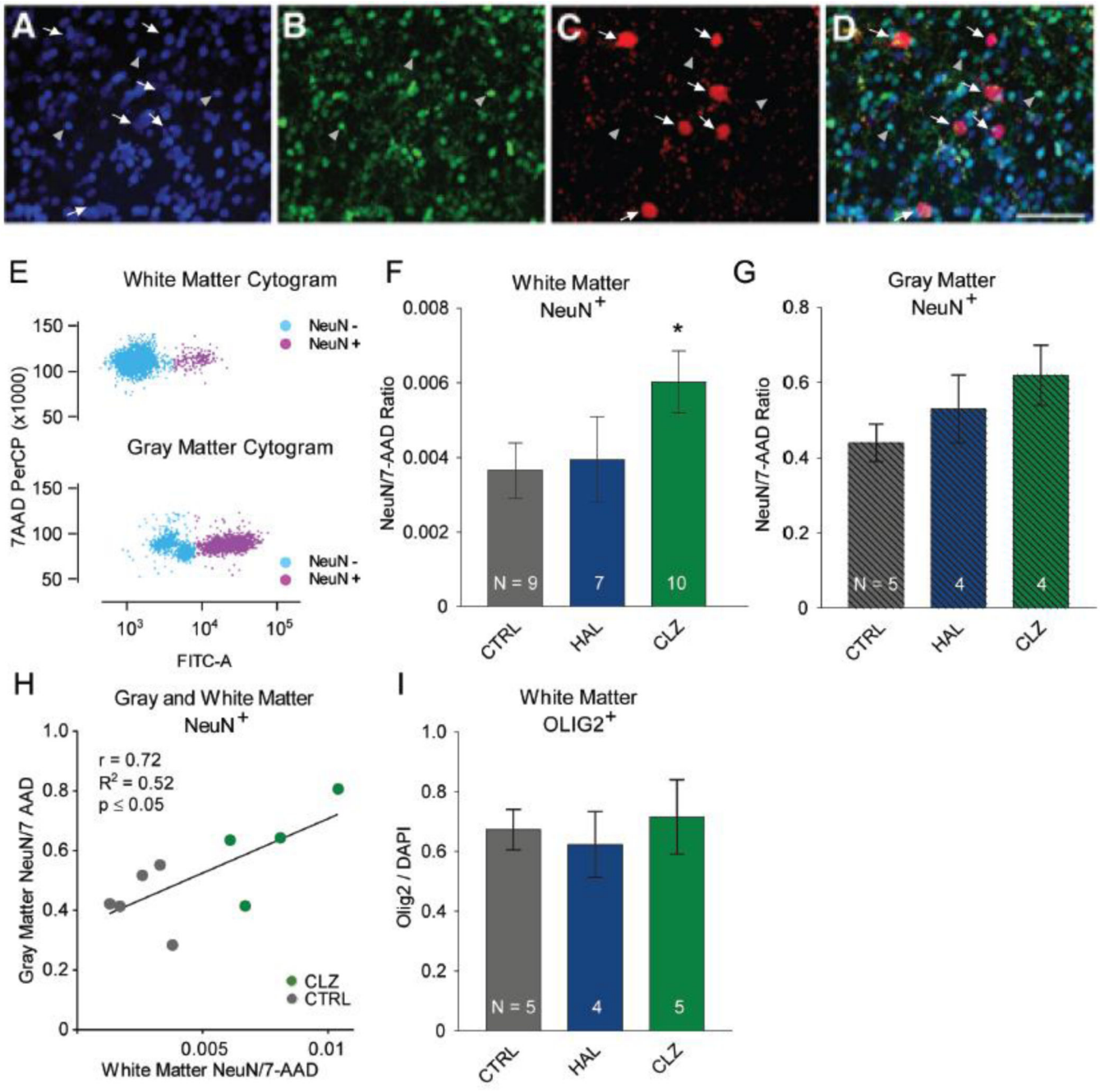

Figure 2. Cell composition in frontal lobe gray and white matter after antipsychotic drug treatment

(**A–D**): Immunofluorescence confocal microscopy from an adult macaque monkey dorsolateral prefrontal white matter. $NeuN^+$, red; $Olig2^+$ green; DAPI counterstain blue. White arrows mark subsets of $NeuN^+$ nuclei and gray arrowheads mark subset of ($OLIG2^+$) nuclei. Note the complete lack of overlap between $NeuN^+$ and $Olig2^+$ cell populations. Scale bar, 10 μm. (**E**): White matter (top) and gray matter (bottom) fluorescence-activated cell sorting (FACS) dot plots after approximately 100,000 sorting events. Nuclei from neuronal and non-neuronal cells were incubated with antibodies against the neuron-specific epitope

NeuN (conjugated to Alexa488) and the fluorescent DNA marker (7AAD). Alexa488-based immunofluorescence (measured in the FITC channel) allows for near-complete separation of neuronal $NeuN^+$ nuclei in purple and non-neuronal $NeuN^-$ nuclei in blue. Note the much higher proportion of $NeuN^+$ nuclei in gray as compared to white matter. (**F, G**): Proportion of $NeuN^+$ nuclei among total pool of nuclei stained with 7-AAD DNA dye in tissue punches from white (**F**) and gray matter (**G**).. Notice increased proportion of $NeuN^+$ nuclei in white and gray matter after clozapine (CLZ) treatment, while haloperidol (HAL)-exposed monkeys show a smaller, non-significant $NeuN^+$ increase. (**H**) Correlation between (y-axis) gray and (x-axis) white matter $NeuN^+$ nuclei in CLZ-treated and CTRL monkeys. (**I**) Bar graphs summarizing proportion of $OLIG2^+$ nuclei in white matter tissue punches, expressed as fraction of nuclei counterstained with nucleophilic dye DAPI.

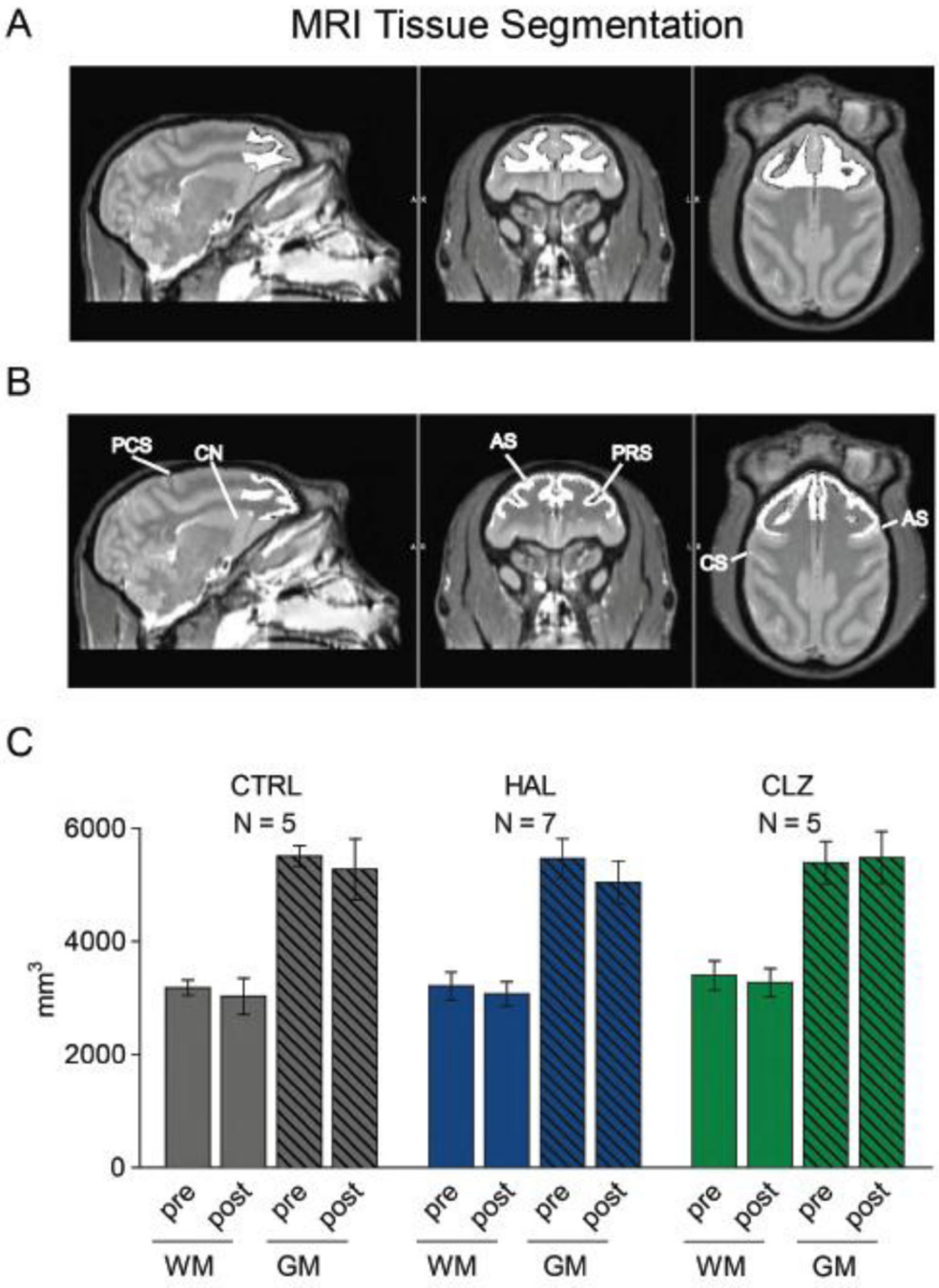

Figure 3. Frontal gray and white matter volumes after 5.5 months of antipsychotic drug treatment

(**A, B**): Representative MRI images (left to right) parasagittal, coronal, horizontal level. Whitened area outlines boundaries of (top) white and (bottom) gray matter portions of dorsolateral frontal lobe used for volumetric studies. AS, arcuate sulcus; CS, central sulcus; PCS, pre-central sulcus; PRS, principal sulcus; CN, caudate nucleus (**C**): Gray and white matter volumes of the dorsolateral frontal lobe after tissue segmentation before ('pre') and 5.5 months ('post') into treatment. There are no differences between (CTRL) controls,

(HAL) haloperidol and (CLZ) clozapine-treated animals. Number (N) of monkeys for each bar as indicated, data shown as mean ± S.E.M.

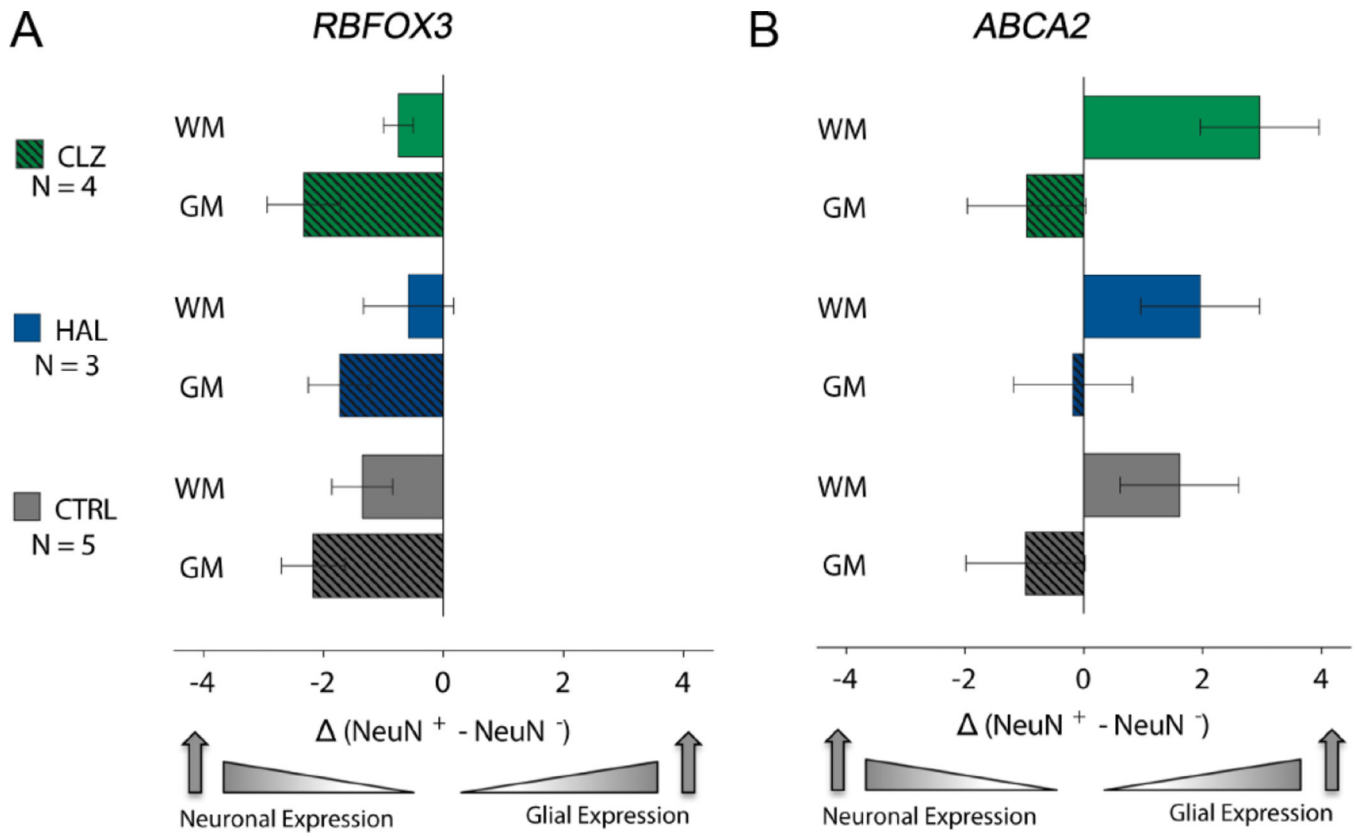

Figure 4. Cell type specific gene expression in white and gray matter

Bar graphs show PCR-based quantification of *RBFOX3* and *ABCA2* RNA extracted from FAC-sorted $NeuN^+$ and $NeuN^-$ nuclei from white and gray matter of CTRL, and HAL- and CLZ-treated animals, as indicated. RNA levels expressed as normalized cycle threshold differences, $NeuN^+$ minus $NeuN^-$ (see Methods). Expression profiles do not show significant differences across groups, with *RBFOX3* levels highest in gray matter $NeuN^+$ nuclei, and *ABCA2* highest in white matter $NeuN^-$ nuclei. Number (N) of monkeys for each bar as indicated and data shown as mean ± S.E.M.

Table 1

Experimental design and cohort demographics

A: Drug treatment								
Group	**N**	**Sex (f/m)**	**Age (yrs)**	**Start Weight (kg)**	**End Weight (kg)**	**Weight Gain (kg)**	**Drug Blood Level (ng/ml)**	**Prolactin (ng/ml)**
CTRL	9	4/5	6.0±0.5	6.0±0.7	7.4±0.8	1.4±0.4	9.6±3.6	9.6±3.6
HAL	7	3/4	5.9±0.3	7.5±1.3	8.3±1.5	0.8±0.3	102.1±24.6	102.1±26.6
CLZ	10	5/5	6.2±0.5	6.2±0.7	7.5±0.7	1.3±0.2	3.8±2.8	4.5±2.8

B: *In vivo* neuroimaging (structural magnetic resonance imaging (MRI) to measure frontal gray and white matter volumes before and after 5.5 months of antipsychotic drug treatment. WM= white matter; GM= gray matter)							
Group	**N**	**Sex (f/m)**	**Age (yrs)**	**Start Volume WM (mm3)**	**End Volume WM (mm3)**	**Start Volume GM (mm3)**	**End Volume GM (mm3)**
CTRL	5	3/2	7.1±0.3	3177	3027	5504	5273
HAL	7	3/4	5.9±0.3	3208	3070	5465	5270
CLZ	5	3/2	7.0±0.3	3395	3268	5383	5480

C: Cell sorting (fluorescence activated nuclei sorting to determine the number of NeuN$^+$ and NeuN$^-$ nuclei in frontal white and gray matter).					
Group	**N**	**Sex (f/m)**	**Age (yrs)**	**NeuN$^+$ nuclei**	**NeuN$^-$ nuclei**
CTRL	9	4/5	5.9±0.5	158	51776
HAL	7	3/4	5.9±0.3	421	123956
CLZ	10	5/5	6.2±0.5	293	45971

D: Molecular fingerprinting (NeuN+ vs. NeuN− specific gene expression in white and gray matter based on PCR-based quantification of *RBFOX3* and *ABCA2*. RNA levels are expressed as Δ= normalized cycle threshold differences).							
Group	**N**	**Sex (f/m)**	**Age (yrs)**	***RBFOX3* (Δ NeuN$^+$ -NeuN$^-$)**		***ABCA2* (Δ NeuN$^+$ -NeuN$^-$)**	
CTRL	5	0/5	5.1±0.6	WM	−1.35	WM	1.61
				GM	−2.17	GM	−0.98
HAL	3	0/3	5.7±0.6	WM	−0.58	WM	1.96

D: Molecular fingerprinting (NeuN+ vs. NeuN− specific gene expression in white and gray matter based on PCR-based quantification of *RBFOX3* and *ABCA2*. RNA levels are expressed as Δ= normalized cycle threshold differences).

Group	N	Sex (f/m)	Age (yrs)	*RBFOX3* (Δ $NeuN^+$ -$NeuN^-$)		*ABCA2* (Δ $NeuN^+$ -$NeuN^-$)	
				GM	−1.73	GM	−0.18
CLZ	4	0/4	5.1±0.7	WM	−0.75	WM	2.96
				GM	−2.33	GM	−0.96